Molecular Cancer Therapeutics

May 2013 - Volume 12 - Issue 5 - Page 553-828

The Journal of Cancer Drug Discovery & Preclinical Development

www.aacrjournals.org

American Association for Cancer Research

Molecular Cancer Therapeutics

Highlights

May 2013 • Volume 12 • Number 5

Selected Articles from This Issue

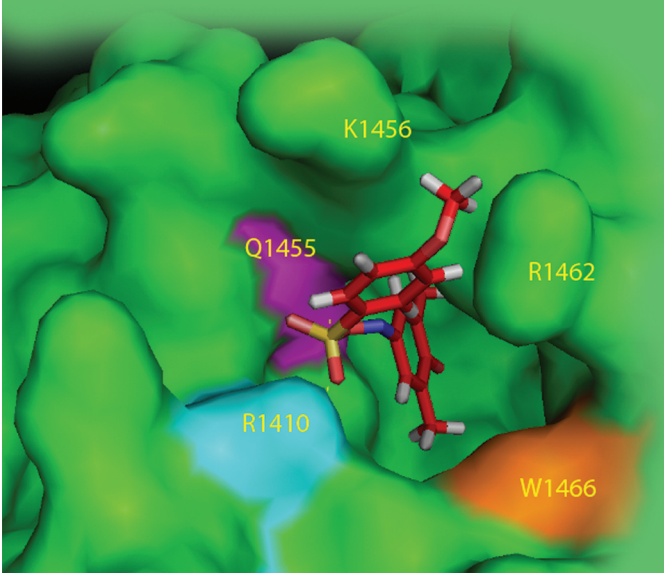

A New Class of Acetyltransferase Inhibitors

Yang *et al.* _____ **Page 610**

Lysine acetyltransferases (KAT) are important for gene expression, metabolism, cell survival, and proliferation. Several KATs such as p300 are overexpressed in cancer and positively linked to tumor progression. Thus, KAT inhibitors have potential for cancer therapy. Using a high-throughput screen campaign, this study identified a new class of potent and specific lead KAT inhibitors that exhibit anticancer activity *in vitro* and *in vivo.* Interestingly, cell lines derived from breast cancer and hematological malignancies are particularly sensitive to these compounds. Together, these data provide a strong rationale for targeting KATs in cancer therapy.

FGFR Inhibitors in Endometrial Cancer

Konecny *et al.* _____ **Page 632**

The identification of activating FGFR2 mutations in endometrial cancer has generated an opportunity for a novel target-based therapy. Konecny and colleagues investigate the therapeutic potential of two new FGFR inhibitors, the multikinase inhibitor dovitinib and the more selective FGFR inhibitor NVP-BGJ398, using comprehensive preclinical models of human endometrial cancer. Both inhibitors show pronounced antitumor activity in FGFR2-mutated endometrial cancer cells and dovitinib, which furthermore targets VEGFR/PDGFR, also showed significant antitumor activity in FGFR2 wild-type endometrial cancer models. Dovitinib and NVP-BGJ398 warrant clinical evaluation in patients with FGFR2-mutated endometrial cancer, and dovitinib may have antitumor activity in endometrial cancer beyond FGFR2 mutated cases.

A Monoclonal Antibody to SFRP2 Inhibits Tumor Growth *In Vivo*

Fontenot *et al.* _____ **Page 685**

SFRP2 is expressed in the vasculature of angiosarcoma and breast cancer, and stimulates angiogenesis via the calcineurin/NFAT pathway. However, there are conflicting reports in the literature as to whether SFRP2 is an antagonist or agonist of β-catenin. The aims of these studies were to assess the effects of SFRP2 antagonism on tumor growth and Wnt-signaling. SFRP2 monoclonal antibody was shown to inhibit tumor growth in angiosarcoma and breast cancer *in vivo,* to inhibit angiogenesis *in vitro* and *in vivo,* and to inhibit activation of β-catenin and NFATc3 in endothelial and tumor cells. Fontenot and colleagues conclude that SFRP2 is a therapeutic target for cancer.

Starving Bevacizumab-Resistant Cancer Cells

Xu *et al.* _____ **Page 717**

Antiangiogenesis therapy has shed new light on cancer treatment, but cancer cells may eventually acquire resistance to anti-VEGF treatment and result in poor outcome. Xu and colleagues provide mechanistic evidence for the involvement of persistent mitochondrial impairment and hyperactive glycolysis in the acquired resistance to anti-VEGF treatment. They treated bevacizumab-resistant colorectal cancer with the glycolysis inhibitior 3-bromopyruvic acid, which significantly suppressed tumor growth both *in vitro* and *in vivo.* These findings elucidate the mechanisms of acquired resistance to anti-VEGF therapy and highlight important therapeutic value for glycolysis inhibitors in the treatment of antiangiogenesis-resistant colorectal cancers.

Contents

Molecular Cancer Therapeutics
The Journal of Cancer Drug Discovery & Preclinical Development
May 2013 • Volume 12 • Number 5

LARGE MOLECULE THERAPEUTICS

CANCER THERAPEUTICS INSIGHTS

TOOLS & TECHNOLOGIES

ABOUT THE COVER

Mitochondria is the powerhouse of cells (structure, green), supplying the majority of ATP that is essential for cell survival. However, cancer cells present a distinct glycolytic metabolism profile (Warburg effect), which is linked to the malignant transformation process. The emerging anti-VEGF therapy fights cancers by starving the energy supplement, but it was found to enhance the Warburg effect and induce even more aggressive phenotypes. Cancer cells with acquired resistance to anti-VEGF therapy display impaired mitochondria structure and hyperactive glycolytic metabolism, which render them vulnerable to glycolysis blockade therapy. For details, see article by Xu and colleagues on page 717.

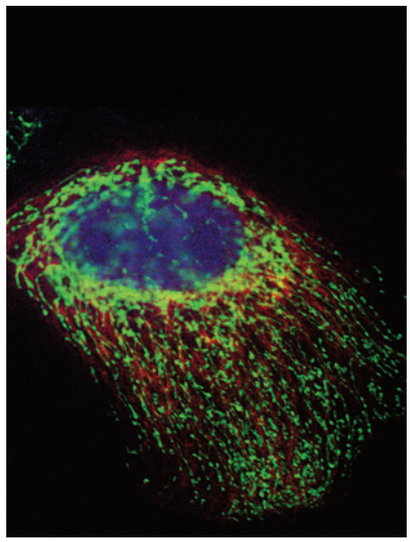

Published OnlineFirst February 20, 2013; DOI: 10.1158/1535-7163.MCT-12-1016-T

Molecular Cancer Therapeutics

Cancer Therapeutics Insights

Colorectal Cancer Cells Refractory to Anti-VEGF Treatment Are Vulnerable to Glycolytic Blockade due to Persistent Impairment of Mitochondria

Jie Xu[1], Jilin Wang[1], Bin Xu[2], Haiyan Ge[3], Xiaolin Zhou[4], and Jing-Yuan Fang[1]

Abstract

Antiangiogenesis therapy has shed new light on cancer treatment, but its effectiveness, especially for overall patient survival, is still controversial. Here, we show that antiangiogenesis treatment causes a persistent suppression of mitochondria biogenesis in colorectal cancer cells, which renders them more sensitive to glycolytic blockade therapy. We first analyzed bevacizumab-resistant colon cancer xenografts by two-dimensional Blue Native/SDS-PAGE and found a serious and persistent loss of mitochondrial protein complex I. Further metabolic assays revealed significantly impaired mitochondrial function and hyperactive glycolysis, which were concomitant with the upregulation of HIF-1 and Hsp70. The treatment of bevacizumab-resistant cells with the glycolysis inhibitor 3-BrPA caused cell senescence *in vitro*. Intraperitoneal injection of 3-BrPA to xenograft mice bearing bevacizumab-resistant cells also resulted in smaller tumor volume and longer survival. These data provide direct evidence for the mitochondrial destruction of bevacizumab-resistant tumor cells and suggest that glycolysis blockade may potentiate the therapeutic effect of antiangiogenesis treatment. *Mol Cancer Ther; 12(5); 717–24. ©2013 AACR.*

Introduction

Colorectal cancer is currently the third most diagnosed cancer in men and the second in women worldwide, and its targeted therapy is under extensively study (1). Given the pivotal role of VEGF-regulated angiogenesis in colorectal cancer progression, anti-VEGF therapeutic strategies hold promise for the treatment of advanced colorectal cancer (2). Bevacizumab, an antibody against VEGF, is currently used in first-line metastatic colorectal cancer treatment in combination with other chemotherapeutic reagents (3). However, the effectiveness of bevacizumab, especially on the overall survival of patients with metastatic colorectal cancer, has been a topic of much debate (4–6). To further improve the effect of anti-VEGF treatment, it is worthy to study the characters of colorectal cancer cells that eventually acquire resistance to antiangiogenesis reagents and develop effective complementary therapeutic strategies.

Accumulating evidence is pointing to a potential role of hypoxic metabolism in the acquired resistance to bevacizumab treatment. The increased dependence of cells on glycolytic pathway for ATP generation is known as one of the most fundamental metabolic alterations during malignant transformation. Hypoxia has been shown to promote tumor progression by accumulating the hypoxia-inducible factor-1α (HIF-1α), which regulates proliferation and angiogenesis (7, 8). Recent studies suggested that a successive hypoxic microenvironment induced by antiangiogenesis treatment can increase the population of tumor stem cells in breast cancer (9) and glioblastoma (10). The anaerobic metabolism of tumors refractory to antiangiogenesis therapy provides a biochemical basis for the design of complementary therapeutic strategies by pharmacological inhibition of glycolysis.

In the present study, we evaluate the extent and reversibility of mitochondria damage in bevacizumab-resistant colorectal cancer cells, aiming to provide mechanistic basis for glycolysis inhibition as a complementary therapeutic strategy. We detected the destruction of mitochondria protein complex I in bevacizumab-resistant (Bev-R) colorectal cancer xenograft and found this characteristic defect still persisted even after Bev-R cells were brought to optimal oxygen-supplied environment. The glycolysis inhibitor 3-bromopyruvic acid (3-BrPA) showed significant inhibitory effect on the growth of bevacizumab-resistant cells both *in vitro* and *in vivo*, suggesting a potential therapeutic value for glycolysis inhibitors to aid anti-VEGF in the treatment of colorectal cancers.

Authors' Affiliations: [1]State Key Laboratory for Oncogenes and Related Genes, GI Division, Shanghai Jiao-Tong University School of Medicine Renji Hospital, Shanghai Institute of Digestive Disease; [2]Department of General Surgery, Shanghai Tenth People's Hospital of Tongji University Medical School; [3]Department of General Surgery, Shanghai East Hospital of Tongji University Medical School; and [4]Department of Neurology, Shanghai First People's Hospital, Shanghai Jiao-Tong University School of Medicine, Shanghai, China

Note: J. Xu and J. Wang contributed equally to the work.

Corresponding Authors: Jie Xu, GI Division, Shanghai Jiao-Tong University School of Medicine Renji Hospital, Shanghai Institute of Digestive Disease, Shanghai 200001, China. Phone: 86-21-53882357; Fax: 86-21-55156787; E-mail: xujieletter@gmail.com; and Jing-Yuan Fang, E-mail: fangjingyuan_new@163.com

doi: 10.1158/1535-7163.MCT-12-1016-T

©2013 American Association for Cancer Research.

Downloaded from mct.aacrjournals.org on May 8, 2013. © 2013 American Association for Cancer Research.

Published OnlineFirst February 20, 2013; DOI: 10.1158/1535-7163.MCT-12-1016-T

Materials and Methods

Reagents and antibodies

Bevacizumab and 3-bromopyruvate were, respectively, purchased from Roche and Sigma-Aldrich. The antibodies specific for mitochondria (MTC02, a mitochondrial marker antibody raised by semipurified mitochondrial preparation), HIF1α (MGC3 mouse monoclonal), Hsp70 (A3A mouse monoclonal), and Vimentin (V9 mouse monoclonal) were purchased from Abcam, and the antibodies for actin (C-2 mouse monoclonal) and MT-ND2 (C-16 rabbit polyclonal) are commercially available from Santa Cruz. The fluorescently labeled secondary antibodies were purchased from Invitrogen.

Cell culture and proliferation assay

The human colon carcinoma LoVo cells were purchased from the American Type Culture Collection and were passaged in our laboratory for less than 6 months. Cells were grown in Dulbecco's Modified Eagle's Medium (DMEM) supplemented with glutamine, pyruvate, antibiotics, and 10% fetal calf serum in a humidified atmosphere containing 5% CO_2 at 37°C. The proliferation of cells was determined based on cell counting. At each time point, cells were trypsinized, diluted, and counted by an automatic cell counter (Scepter, Millipore).

Mitochondrial function assay

Mitochondrial function assay was conducted according to the product manual of ToxGlo assay (Promega). Production of ATP via glycolysis using galactose-containing media yields no net ATP, and cells primarily use mitochondrial oxidative phosphorylation to produce ATP. Therefore, the level of ATP can well reflect the function of mitochondria in cells cultured with galactose-containing media (11, 12). To measure mitochondrial function, equal number of $LoVo^{Bev\text{-}R}$ and control cells was plated into 96-well plates, and 10 mmol/L galactose was used to replace glucose in the media to enhance mitochondrial metabolism. The amount of dead cells was quantified by addition of a fluorogenic peptide substrate (bis-AAF-R110), which cannot cross the intact membrane and only measures dead cell protease activity. The mitochondrial function was then measured by quantification of the generated ATP using a luminescent assay.

Glycolytic activity assay

Glycolysis of cells was determined by measuring the amount of lactate, the end product of glycolysis, using a commercially available kit (#600450, Cayman Chemical Company). The assay was conducted according to the product manual. Briefly, cells were seeded in a 96-well plate at a density of 50,000 cells/well in DMEM containing 25 mmol/L glucose, 10% FBS. After 24 hours, culture supernatant (10 μL) was removed from each well and added to reaction solution. The mixture was incubated with gentle shaking on an orbital shaker for 30 minutes at room temperature, and the absorbance at 490 nm was detected with a plate reader.

Western blot analysis

Cell lysate proteins were separated by SDS-PAGE (10% gels) and transferred to nitrocellulose membranes. Protein amounts were quantified using the Bradford method, and equal protein amounts were loaded to the gel. Membranes were blocked in Tris-buffered saline with 0.05% Tween 20 (TBST) containing 5% nonfat dry milk powder for 1 hour. Western blots were probed with primary antibodies for 1 hour, washed 3 times with TBST, and then incubated with the appropriate secondary antibodies for 30 minutes. Membranes were then washed with TBST 3 times, before developing with SuperSignal West Dura chemiluminescent substrate.

Immunofluorescent staining

Cells were removed from incubator and washed with PBS, followed by fixation using 4% formalin for 15 minutes. After permeabilization and blocking with 0.2% Triton X-100 and 1% BSA in PBS for 1 hour, the first antibody was diluted at 1:100 and incubated with the slide for 40 minutes. The secondary antibodies were diluted at 1:1,000 and incubated with the slides for 15 minutes. The fluorescent images were taken using a confocal microscope (Nikon).

Quantitative reverse transcription PCR

Quantitative reverse transcription PCR (qRT-PCR) was carried out using the following oligonucleotides and PCR conditions: 2 minutes at 95°C (20 seconds at 95°C, 20 seconds at the annealing temp, and 30 seconds at 72°C) × 35, and 10 minutes at 72°C. Primers were as follows: actin, forward: 5′-CATCACTATTGGCAACGAG-C-3′, reverse: 5′-ACGCAGCTCAGTAACAGTCC-3′; Hsp70, forward: 5′-GCCGAGAAGGACGAGTTTGA-3′, reverse: 5′-TCCGCTGATGATGGGGTTAC-3′; HIF-1α, forward: 5′-CGTTCCTTCGATCAGTTGTC-3′, reverse: 5′-TCAGTGGTGGCAGTGGTAGT-3′; and MT-ND, forward: 5′-GCCCTAGAAATAAACATGCTA-3′, reverse: 5′- GGGCTATTCCTAGTTTTATT-3′.

Creation of xenograft model

All animal experiments were carried out in the experimental animal platform of Tongji University (Shanghai, China). Protocols were conducted in accordance with Guidance Suggestions for the Care and Use of Laboratory Animals, formulated by The Ministry of Science and Technology of the People's Republic of China. Nude mice were grafted subcutaneously in the left flank with 5×10^6 LoVo cells in 0.3 mL of sterile normal saline solution. Mice were randomized into control and experimental groups (each containing 5 mice) when the tumor volume reached approximately 100 mm^3. Tumors were measured with a caliper and calculated using the formula: $0.5 \times a \times b^2$, where a was the length and b was the width of the tumor.

Drug treatment

In the experimental and control groups, bevacizumab (5 mg/kg) and PBS were respectively injected intraperitoneally twice a week. Tumors were measured by calipers

Downloaded from mct.aacrjournals.org on May 8, 2013. © 2013 American Association for Cancer Research.

Published OnlineFirst February 20, 2013; DOI: 10.1158/1535-7163.MCT-12-1016-T

twice weekly. At the end of drug treatment, the mice were humanely euthanized and tumors were, respectively, harvested. Tumor tissues were dissociated mechanically and enzymatically to obtain a single-cell suspension. Tumors were minced by scalpel and incubated in Medium 199 (Invitrogen) mixed with collagenase/hyaluronidase (Sigma Aldrich) at 37°C for 60 minutes. The tissues were further dissociated by pipette trituration and then passed through a 40-μm nylon mesh to produce a single-cell suspension, which was used for subsequent culture and treatments. Cells derived from experimental and control groups of xenografts were, respectively, mixed and incubated (named as $LoVo^{Bev\text{-}R}$ and $LoVo^{control}$ cells).

For *in vitro* treatment with 3-BrPA, xenograft-derived cells ($LoVo^{Bev\text{-}R}$ and $LoVo^{control}$) were, respectively, cultured in media containing 150 μmol/L of 3-BrPA. For *in vivo* 3-BrPA treatment, mice implanted with $LoVo^{Bev\text{-}R}$ and $LoVo^{control}$ cells were injected intraperitoneally 5 mg/kg 3-BrPA once per day when the xenograft volume reached 300 mm^3. The tumor volume was measured every 2 days after the first 3-BrPA injection.

Two-dimensional BN/SDS-PAGE

The two-dimensional (2D) BN/SDS-PAGE was conducted according to the product manual of the Native-PAGE Novex Bis-Tris Gel System (Invitrogen). Briefly, the 1D Blue native-PAGE was conducted with a buffer system containing Coomassie G250 but without SDS. Cells were lysed using 18 mmol/L 3-[(3-cholamidopropyl)dimethylammonio]-1-propanesulfonic acid (CHAPS) in TBS with DNase and protease inhibitors (Roche) for 30 minutes on ice, and a sample buffer containing 10% glycerol and 1% Coomassie was added to the lysate before electrophoresis. The strip of the interested lane was cut, incubated in 1% SDS for 10 minutes, and assembled into a one-well SDS gel. The 2D electrophoresis was conducted in MES running buffer containing 1% SDS. The resultant 2D gel was stained using a silver staining kit (Bio-Rad) according to the product manual or transferred to polyvinylidene difluoride (PVDF) membranes and stained using Coomassie. Stained proteins of interest were identified using N-terminal (Edman) sequencing in GeneCore proteomics service facility.

Results

Bevacizumab treatment led to mitochondria destruction and dysfunction

To mimic the acquired resistance to antiangiogenesis treatment of colorectal cancer cells, we implanted the LoVo colorectal cancer cells to nude mice and treated the established xenograft with 5 mg/kg bevacizumab (or PBS as control) intraperitoneally twice a week. The treatment of bevacizumab initially suppressed the growth of xenograft, but in the late phase of treatment, the tumor size started to increase again, indicating an acquired resistance to anti-VEGF therapy. The bevacizumab-resistant xenografts were excised, minced, and digested with an enzyme mixture to obtain single-cell suspensions ($LoVo^{Bev\text{-}R}$). The cells derived from 5 bevacizumab-resistant xenografts were mixed and cultured under an optimized oxygen-supplied condition for 3 weeks, followed by 2D Blue Native/SDS-PAGE (2D BN/SDS-PAGE) to examine the status of mitochondrial protein complexes. Cells were also derived from xenografts in the control group and analyzed using the same procedure. The 1D Blue Native-PAGE fractionated protein complexes without disrupting native protein binding, whereas the 2D SDS-PAGE broke down the complexes to display individual subunits. As shown in Fig. 1A and B, the $LoVo^{Bev\text{-}R}$ cells showed dramatic decrease of a protein complex with MW of over 1,000kda as compared with LoVo cells from control xenografts. The 2D PAGE revealed multiple subunits with various molecular sizes that constituted this large complex (Fig. 1C and D). We blotted these proteins to PVDF membrane and conducted N-terminal protein sequencing on 2 selected spots, which turned out to be MT-ND2 and NDUFV2, 2 components of the mitochondria protein complex I (NADH dehydrogenase; Fig. 1E and F).

To probe the status of mitochondria in $LoVo^{Bev\text{-}R}$ cells, we conducted immunofluorescence using a specific marker for mitochondria. A substantial decrease of mitochondria content was detected in $LoVo^{Bev\text{-}R}$ cells as compared with control LoVo cells, as indicated by the lower staining intensity and fewer mitochondrial structures in $LoVo^{Bev\text{-}R}$ cells (Fig. 2A). Moreover, the structure of the mitochondria in $LoVo^{Bev\text{-}R}$ cells was punctuate-like, and this was in contrast to the thinned, filamentous morphology of control LoVo cells (Fig. 2A). Combining the result of 2D PAGE, these data suggested a substantial disorder of the mitochondria structure in bevacizumab-resistant LoVo cells.

Suppression of angiogenesis potentiated glycolytic activity of cancer cells

Given the vital role of NADH dehydrogenase (complex I) in mitochondrial electron transport chain, we examined the extent of mitochondria impairment in $LoVo^{Bev\text{-}R}$ cells. The mitochondria functional assay suggested a dramatic decrease of mitochondria activity in $LoVo^{Bev\text{-}R}$ cells, which only accounted for 10% of the level in control cells (Fig. 2B). We further determined the glycolytic activity of $LoVo^{Bev\text{-}R}$ cells and found it increased by 5-folds as compared with control LoVo cells (Fig. 2C). Western blot and qRT-PCR assays showed decreased level of MT-ND2 in $LoVo^{Bev\text{-}R}$ cells (Fig. 3), which was consistent with the result from 2D PAGE. Moreover, the mRNA and protein levels of HIF-1 and Hsp70 were significantly increased in $LoVo^{Bev\text{-}R}$ cells (Fig. 3), suggesting that HIF-1 may be relevant to the activation of glycolytic pathway. Note these results were obtained from $LoVo^{Bev\text{-}R}$ cells cultured for 3 weeks under optimal oxygen-supplied condition. The persistence of increased glycolysis caused by anti-VEGF treatment supports the model that cells progressively evolve

Downloaded from mct.aacrjournals.org on May 8, 2013. © 2013 American Association for Cancer Research.

Published OnlineFirst February 20, 2013; DOI: 10.1158/1535-7163.MCT-12-1016-T

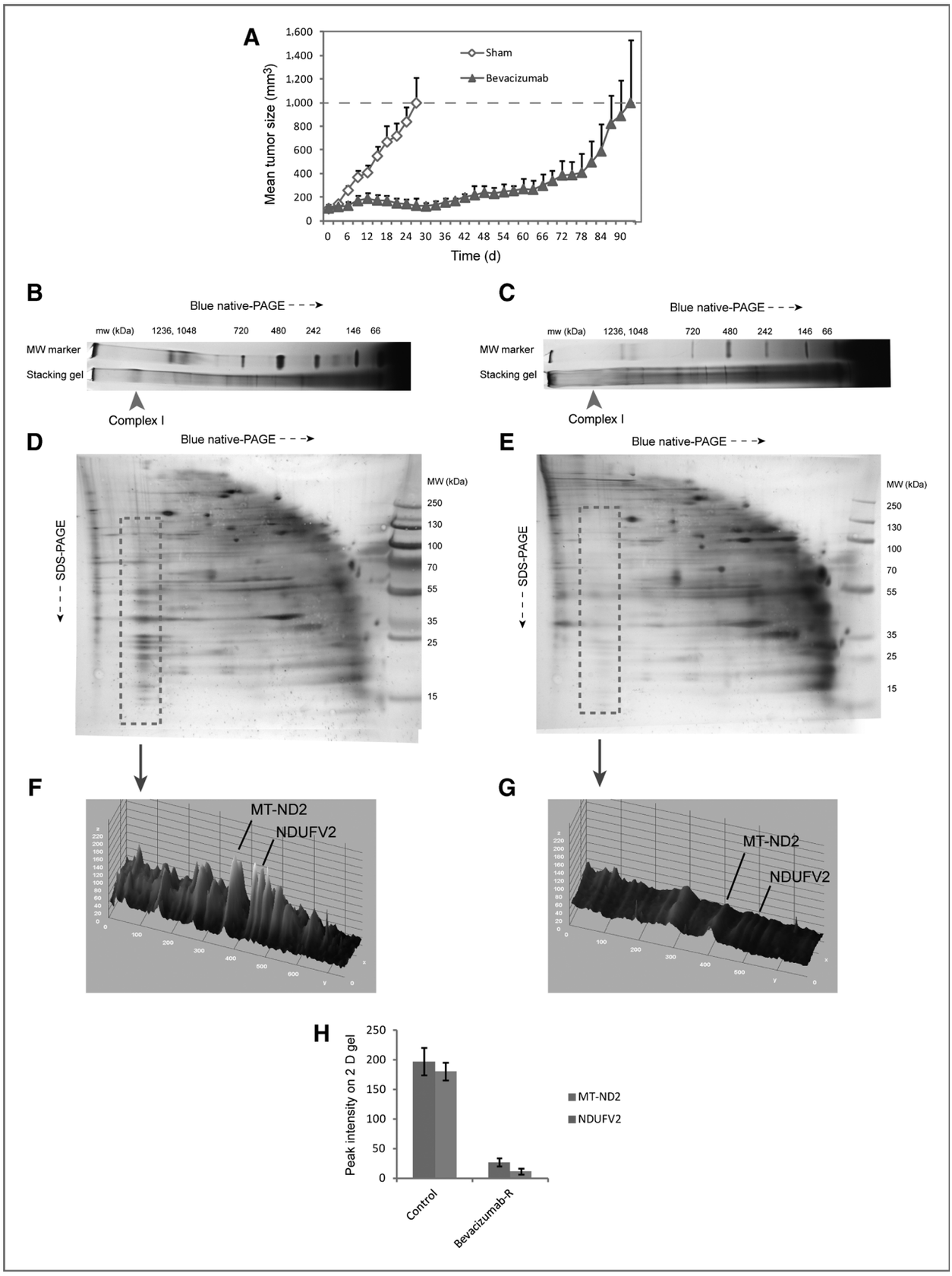

Downloaded from mct.aacrjournals.org on May 8, 2013. © 2013 American Association for Cancer Research.

Published OnlineFirst February 20, 2013; DOI: 10.1158/1535-7163.MCT-12-1016-T

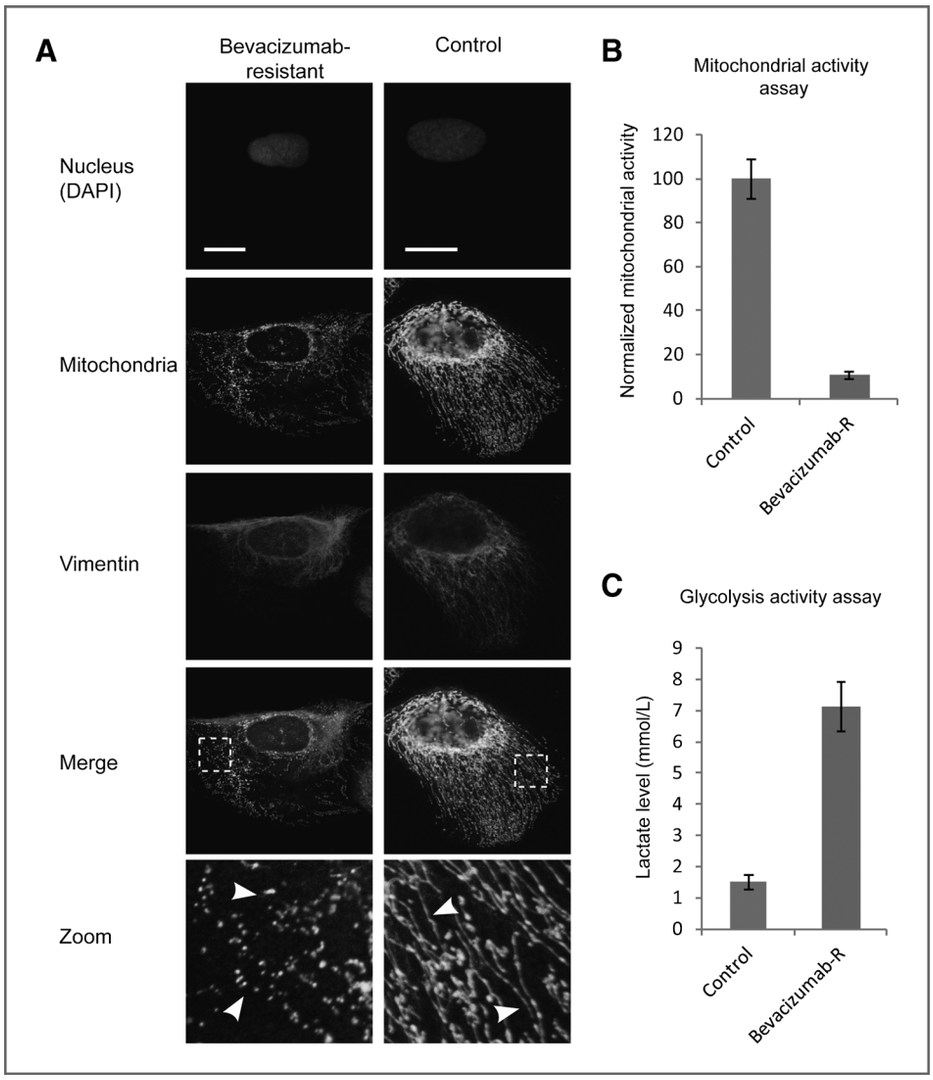

Figure 2. Impaired mitochondria structure and function in LoVo^{Bev-R} cells. A, the morphology of mitochondria in control and LoVo^{Bev-R} cells detected by immunofluorescence. A mitochondria-specific antibody raised by semipurified mitochondrial preparation (MTC02, Abcam) was used to label mitochondria in green, and vimentin was stained using a monoclonal antibody in red. Cell nucleus was stained by DAPI in blue. The scale bars indicate 10 μmol/L. The white dashed box marks the region that is zoomed in the lowest panel. The white arrowheads indicate the filamentous morphology of mitochondria in the control cells and the fragmented punctuate-like structure of mitochondria in LoVo^{Bev-R} cells. B, the mitochondria functional assay of control cells and LoVo^{Bev-R} cells. The ATP generated by cells was converted to luminescent signal, which was normalized to present the percentage of activity as compared with the control cells. As a control, the "dead cell proteases" activities in both groups were at baseline level. The data represent the mean ± SD of 4 independent experiments. C, glycolysis activity assay for control cells and LoVo^{Bev-R} cells. The measured values were normalized to show the percentage of activity as compared with LoVo^{Bev-R} cells. The data represent the mean ± SD of 4 independent experiments.

toward malignancy during adaptation to the hypoxic microenvironment (13).

Glycolytic blockade induced cell senescence and growth suppression *in vitro*

As the vital energy source that supported the fast proliferation of LoVo^{Bev-R} cells was glycolysis-generated ATP, it is thus plausible to use glycolysis inhibitors to suppress the growth of these hypoxia-adapted cells. The small compound 3-BrPA, a synthetic brominated derivate of pyruvic acid, is a potent inhibitor of glycolysis capable of inducing severe ATP reduction and cell death in cancer cells with mitochondrial defects or under hypoxic conditions (14, 15). A recent study suggested that 3-BrPA could induce the covalent modification of HKII protein and directly trigger its dissociation from mitochondria, thus provided a potential mechanism for the anti-glycolytic effect of 3-BrPA (16). We treated the LoVo^{Bev-R} cells *in vitro* using 150 μmol/L 3-BrPA and analyzed the effect of glycolysis inhibition on cell

Figure 1. Bevacizumab-resistant LoVo cells (LoVo^{Bev-R}) loss mitochondria protein complex I. A, the size of xenograft tumors in the bevacizumab group and control groups. The tumors treated with bevacizumab showed slower growth rate as compared with the control group, but in the late phase of treatment, these tumors acquire resistance to anti-VEGF treatment and started to progress again. B and C, Blue-Native PAGE of control LoVo cells and LoVo^{Bev-R} cells. The upper lane presents molecular weight standard (NativeMark) stained with Coomassie blue, and the lower lane indicates the protein complexes fractionated by the Blue Native-PAGE. The arrowhead labels the band that corresponds to mitochondria protein complex I (NADH dehydrogenase), which is absent in LoVo^{Bev-R} cells. D and E, 2D BN/SDS-PAGE of control LoVo cells and LoVo^{Bev-R} cells. The gel was blotted to PVDF membrane and stained with Coomassie blue. The dashed box indicates the subunits of mitochondria complex I. F and G, 3D intensity profiling of stained protein complex I subunits. The 2 abundant subunits were identified by N-terminal protein sequencing as MT-ND2 and NDUFV2, which were absent in the LoVo^{Bev-R} cells. H, statistics of MT-ND2 and NDUFV2 intensity in the 2-D gel. Three independent experiments were carried out to analyze the levels of MT-ND2 and NDUFV2 in LoVo^{Bev-R} and control cells. The difference is statistically significant ($P < 0.01$; Student t test).

Downloaded from mct.aacrjournals.org on May 8, 2013. © 2013 American Association for Cancer Research.

Published OnlineFirst February 20, 2013; DOI: 10.1158/1535-7163.MCT-12-1016-T

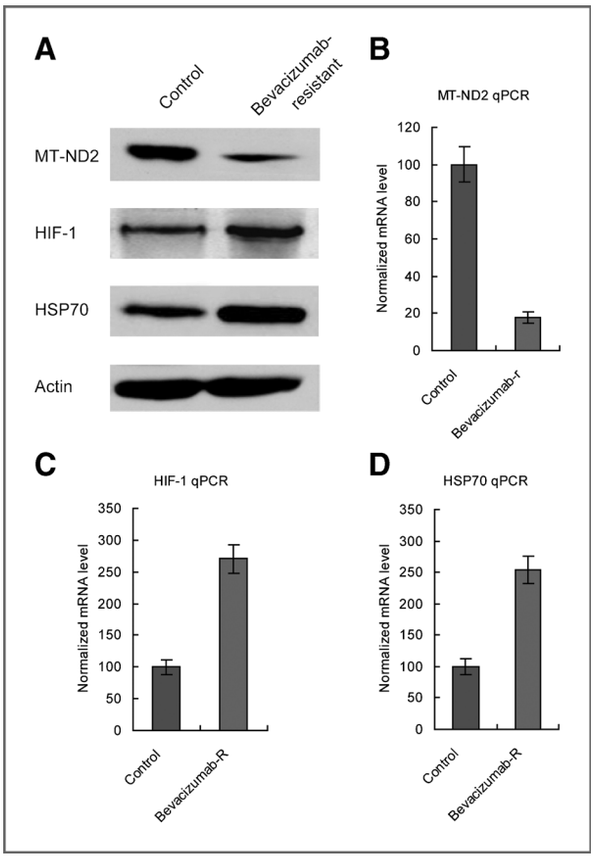

Figure 3. Expression levels of MT-ND2, HIF-1 and Hsp70 in control and LoVo^{Bev-R} cells. A, Western blot analysis of control and LoVo^{Bev-R} cells. The cells were lysed and analyzed by SDS-PAGE, and the blotted membrane was probed with antibody for MT-ND2, HIF-1α, Hsp70, and actin to show the protein expression level. B–D, mRNA levels of MT-ND2, HIF-1α, and Hsp70 as determined by qRT-PCR. Total mRNA was isolated from control and LoVo^{Bev-R} cells, and cDNAs were synthesized using random primers. The levels of MT-ND2, HIF-1, and Hsp70 mRNA were determined by qPCR. All values were normalized with the expression level of actin.

proliferation. The presence of 3-BrPA induced progressive senescent morphology of LoVo^{Bev-R} cells with the formation of large and flat cell bodies (Fig. 4A). After 8 days of incubation, all cells were out of the cell cycle and showed giant nuclei within enormous cytoplasmic masses (Fig. 4A). Consistently, cell number counting also suggested that LoVo^{Bev-R} cells stopped proliferation after 6 to 8 days of incubation with 3-BrPA. On the contrary, the control LoVo cells without preselection by bevacizumab showed few senescent cells till the end of incubation, and the proliferation rate of control LoVo cells was also significantly faster than that of LoVo^{Bev-R} cells (Fig. 4B).

3-BrPA reduced tumor size and improved survival of xenograft-transplanted mice

We further tested the effect of 3-BrPA on LoVo^{Bev-R} cells in a xenograft mouse model. The LoVo^{Bev-R} and control cells were respectively implanted into the left flank of 15 nude mice, and 3-BrPA was injected intraperitoneally after the xenograft volume reached 300 mm^3. We measured tumor sizes 6 days after injection of 3-BrPA and found that the LoVo^{Bev-R} xenografts showed very limited growth (~350 mm^3). On the contrary, the tumor sizes in the control group increased by over one fold (Fig. 4C and D). Moreover, the survival of mice bearing LoVo^{Bev-R} xenografts was significantly longer than those control mice, suggesting a consistent effect of 3-BrPA as observed *in vitro*.

Discussion

Bevacizumab is the first-in-class VEGF inhibitor that was initially approved by the U.S. Food and Drug Administration in 2004 for the treatment of metastatic colon cancer and other solid tumors. However, recent clinical data concluded that incorporating bevacizumab into adjuvant regimens does not prolong disease-free survival (DFS) or overall survival (OS) of patients with colorectal cancers (17). In this study, we provide mechanistic evidence for the involvement of persistent mitochondrial impairment in the acquired resistance to anti-VEGF treatment. The mitochondria of LoVo^{Bev-R} cells showed severe loss of the mitochondrial complex I (NADH dehydrogenase) as revealed by the 2D BN/SDS-PAGE. NADH dehydrogenase is the first enzyme (complex I) of the mitochondrial electron transport chain, and its proper functionality is vital for ATP generation through the aerobic respiration pathway. We also showed by immunofluorescence that the amount of mitochondria significantly decreased in LoVo^{Bev-R} cells, concomitant with the loss of filamentous morphology and the appearance of fragmented, punctuate-like structure of mitochondria. It was thus not surprising that the mitochondrial function in LoVo^{Bev-R} cells was dramatically decreased as compared with control cells. However, the fast proliferation of LoVo^{Bev-R} cells *in vitro* suggested they might consume comparable amount of ATP as the control cells. This was explained by the hyperactivation of glycolysis in the LoVo^{Bev-R} cells, thus suggesting a substantial shift of metabolistic pathway in bevacizumab-resistant colorectal cancer cells.

The dependence of LoVo^{Bev-R} cells on glycolytic metabolism was persistent and was not affected by the supplement of oxygen in the culture condition. This could be explained by the sustained upregulation of HIF-1α, which is known to stimulate expression of glycolytic enzymes and decreases reliance on mitochondrial oxidative phosphorylation in tumor cells (18). Moreover, both Western blotting and qPCR suggested the upregulation of Hsp70 in the bevacizumab-resistant LoVo cells. The molecular chaperone Hsp70 is a transcriptional target of HIF-1, which can help cancer cells to overcome hypoxic stress and survive (19). These findings provided mechanistic insight into how colorectal cancer cells evade from anti-VEGF treatment and evolve toward malignant phenotypes.

The severe and persistent dependence of bevacizumab-resistant cells on glycolytic metabolism provides a venue for complementary therapeutic strategy. Our

Downloaded from mct.aacrjournals.org on May 8, 2013. © 2013 American Association for Cancer Research.

Published OnlineFirst February 20, 2013; DOI: 10.1158/1535-7163.MCT-12-1016-T

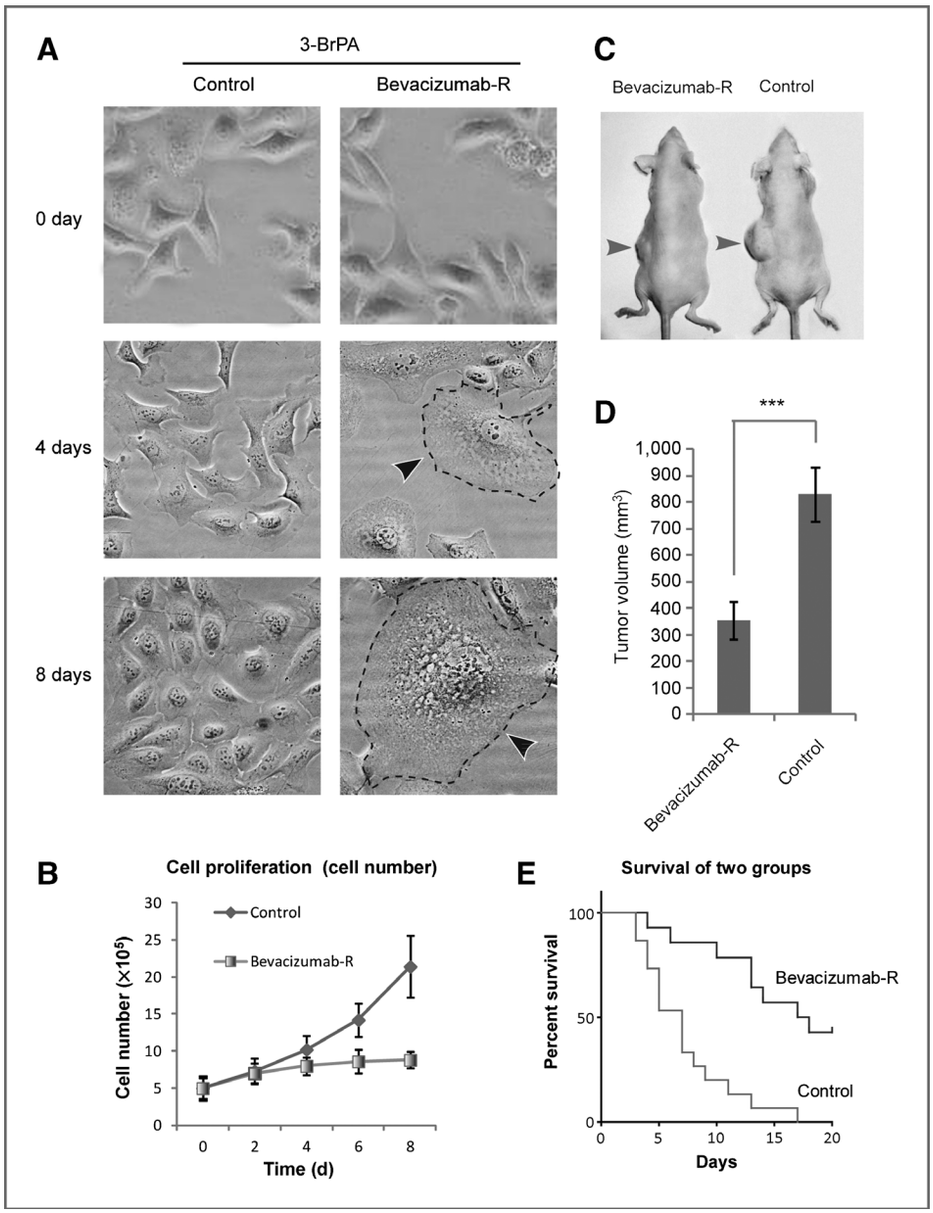

Figure 4. Inhibitory effect of 3-BrPA on the proliferation of LoVo$^{Bev\text{-}R}$ cells. A, morphologic change of control and LoVo$^{Bev\text{-}R}$ cells incubated with 3-BrPA. The regions surrounded by dashed lines indicate cells with senescent morphology. B, proliferation of control and LoVo$^{Bev\text{-}R}$ cells treated by 3-BrPA as determined by cell number counting. The cell number was determined every 2 days, and the data represent the mean ± SD of 4 independent experiments. C, representative images of xenograft mice treated by 3-BrPA. The intraperitoneal injection of 3-BrPA resulted in smaller tumor size for the LoVo$^{Bev\text{-}R}$ xenograft (arrowhead on the left). D, the tumor volume of control and LoVo$^{Bev\text{-}R}$ xenografts treated by 3-BrPA. Data represent the mean ± SD. ***, $P < 0.01$ (Student t test). E, survival curve of mice bearing control and LoVo$^{Bev\text{-}R}$ xenografts treated with 3-BrPA. Each group contained 15 mice, and the survival of mice was followed for 20 days after the first treatment of 3-BrPA. The survival of LoVo$^{Bev\text{-}R}$ xenograft mice were significantly longer than that of control mice ($P < 0.001$; Kaplan–Meier).

data suggested that the glycolytic inhibitor, 3-BrPA, could significantly suppress the proliferation of LoVo$^{Bev\text{-}R}$ cells and induce their senescence *in vitro*. The therapeutic effect of 3-BrPA has been reported previously in many cancers (20), and here we show that 3-BrPA is especially effective against the colorectal cancer cells that have acquired resistance to anti-VEGF therapy. The hypoxic microenvironment induced by bevacizumab may select cells that have evolved with hyperactive glycolytic metabolism, and blockade of glycolysis could thus deprive the major source of ATP and drive cells to senescence. Our *in vivo* data showed that injection of 3-BrPA to mice carrying bevacizumab-resistant colorectal cancer tumor resulted in significantly decreased tumor volume and longer survival, thus indicating glycolysis inhibition as a potential complementary strategy for antiangiogenesis therapy.

Taken together, our study provided direct evidence for the involvement of persistent mitochondria impairment and hyperactive glycolysis in the acquired resistance of colorectal cancer cells against anti-VEGFtreatment. We also showed that glycolysis blockade strongly suppressed the proliferation of colorectal cancer cells that were refractory to bevacizumab treatment. In future studies, it is interesting to examine the effects of other glycolysis inhibitors on bevacizumab-resistant colorectal cancer cells. It would also be meaningful to study whether a synergetic therapeutic effect could be achieved by combination of bevacizumab and 3-BrPA in clinical colorectal cancer cases.

Downloaded from mct.aacrjournals.org on May 8, 2013. © 2013 American Association for Cancer Research.

Published OnlineFirst February 20, 2013; DOI: 10.1158/1535-7163.MCT-12-1016-T

Disclosure of Potential Conflicts of Interest

No potential conflicts of interest were disclosed.

Authors' Contributions

Conception and design: J. Xu
Development of methodology: J. Xu, J. Wang
Acquisition of data (provided animals, acquired and managed patients, provided facilities, etc.): J. Xu, J.-Y. Fang
Analysis and interpretation of data (e.g., statistical analysis, biostatistics, computational analysis): J. Xu, X. Zhou
Writing, review, and/or revision of the manuscript: J. Xu, J. Wang, B. Xu, H. Ge, J.-Y. Fang
Administrative, technical, or material support (i.e., reporting or organizing data, constructing databases): X. Zhou
Study supervision: J.-Y. Fang

Grant Support

This research project is supported by National Basic Research Program of China 973 program Grant (No.2010CB5293), the National High Technology Research, and Development Program of China (863 Program; Grant No. 2012AA02A504) to J.-Y. Fang; National Natural Science Foundation of China (Grants No. 81000861 and 81272383) and Shanghai Natural Science Foundation (Grant No. 12ZR1417900) to J. Xu; and National Natural Science Foundation of China (No. 81200976) to X. Zhou.

The costs of publication of this article were defrayed in part by the payment of page charges. This article must therefore be hereby marked *advertisement* in accordance with 18 U.S.C. Section 1734 solely to indicate this fact.

Received December 20, 2012; revised January 31, 2013; accepted February 4, 2013; published OnlineFirst February 20, 2013.

References

1. Jemal A, Bray F, Center MM, Ferlay J, Ward E, Forman D. Global cancer statistics. CA Cancer J Clin 2011;61:69–90.
2. Grothey A, Galanis E. Targeting angiogenesis: progress with anti-VEGF treatment with large molecules. Nat Rev Clin Oncol 2009;6:507–18.
3. Strickler JH, Hurwitz HI. Bevacizumab-based therapies in the first-line treatment of metastatic colorectal cancer. Oncologist 2012;17:513–24.
4. Macedo LT, da Costa Lima AB, Sasse AD. Addition of bevacizumab to first-line chemotherapy in advanced colorectal cancer: a systematic review and meta-analysis, with emphasis on chemotherapy subgroups. BMC Cancer 2012;12:89.
5. Terme M, Pernot S, Marcheteau E, Sandoval F, Benhamouda N, Colussi O, et al. VEGFA-VEGFR pathway blockade inhibits tumor-induced regulatory T-cell proliferation in colorectal cancer. Cancer Res 2013;73:539–49.
6. Montero AJ, Vogel C. Fighting fire with fire: rekindling the bevacizumab debate. N Engl J Med 2012;366:374–5.
7. Trisciuoglio D, Gabellini C, Desideri M, Ragazzoni Y, De Luca T, Ziparo E, et al. Involvement of BH4 domain of bcl-2 in the regulation of HIF-1-mediated VEGF expression in hypoxic tumor cells. Cell Death Differ 2011;18:1024–35.
8. Morine Y, Shimada M, Utsunomiya T, Imura S, Ikemoto T, Mori H, et al. Hypoxia inducible factor expression in intrahepatic cholangiocarcinoma. Hepatogastroenterology 2011;58:1439–44.
9. Conley SJ, Gheordunescu E, Kakarala P, Newman B, Korkaya H, Heath AN, et al. Antiangiogenic agents increase breast cancer stem cells via the generation of tumor hypoxia. Proc Natl Acad Sci U S A 2012;109:2784–9.
10. Keunen O, Johansson M, Oudin A, Sanzey M, Rahim SA, Fack F, et al. Anti-VEGF treatment reduces blood supply and increases tumor cell invasion in glioblastoma. Proc Natl Acad Sci U S A 2011;108:3749–54.
11. Aguer C, Gambarotta D, Mailloux RJ, Moffat C, Dent R, McPherson R, et al. Galactose enhances oxidative metabolism and reveals mitochondrial dysfunction in human primary muscle cells. PLoS ONE 2011;6:e28536.
12. Marroquin LD, Hynes J, Dykens JA, Jamieson JD, Will Y. Circumventing the Crabtree effect: replacing media glucose with galactose increases susceptibility of HepG2 cells to mitochondrial toxicants. Toxicol Sci 2007;97:539–47.
13. Fang JS, Gillies RD, Gatenby RA. Adaptation to hypoxia and acidosis in carcinogenesis and tumor progression. Semin Cancer Biol 2008;18:330–7.
14. Nelson K. 3-Bromopyruvate kills cancer cells in animals. Lancet Oncol 2002;3:524.
15. Birsoy K, Wang T, Possemato R, Yilmaz OH, Koch CE, Chen WW, et al. MCT1-mediated transport of a toxic molecule is an effective strategy for targeting glycolytic tumors. Nat Genet 2012;45:104–8.
16. Chen Z, Zhang H, Lu W, Huang P. Role of mitochondria-associated hexokinase II in cancer cell death induced by 3-bromopyruvate. Biochim Biophys Acta 2009;1787:553–60.
17. Shojaei F. Anti-angiogenesis therapy in cancer: current challenges and future perspectives. Cancer Lett 2012;320:130–7.
18. Shaw RJ. Glucose metabolism and cancer. Curr Opin Cell Biol 2006;18:598–608.
19. Huang WJ, Xia LM, Zhu F, Huang B, Zhou C, Zhu HF, et al. Transcriptional upregulation of HSP70-2 by HIF-1 in cancer cells in response to hypoxia. Int J Cancer 2009;124:298–305.
20. Ganapathy-Kanniappan S, Vali M, Kunjithapatham R, Buijs M, Syed LH, Rao PP, et al. 3-bromopyruvate: a new targeted antiglycolytic agent and a promise for cancer therapy. Curr Pharm Biotechnol 2010;11:510–7.

Downloaded from mct.aacrjournals.org on May 8, 2013. © 2013 American Association for Cancer Research.